International Journal Of
Industrial Electronics Control and Optimization
Print ISSN: 3517-2645
Online ISSN: 3568-2645
Homepage: https://ieco.usb.ac.ir/

Fractional-Order Variable Structure Equations In Robust Control

Ebrahim Abbaszadeh-Soorami[1] | Mohammad Haddad-Zarif[1]

Department of Electrical and Robotic Engineering, Shahrood University of technology, Shahrood, Iran.[1]
Corresponding author's email: mhzarif@shahroodut.ac.ir

Article Info

Article type:
Research Article

Article history:
Received: 23 January 2023
Received in: 3 May 2023
Accepted: 23 May 2023
Published online: 5 July 2023

Keywords:
Fractional-order,
Robust Control,
Fast Response,
Variable Structure Control.

ABSTRACT

This work is trying to introduce a fractional order floated pole controller as a fast and robust approach. We designed a robust variable structure control that yields a continuous and constrained control signal, also a fast response in the presence of model uncertainties and external disturbances. In the proposed controller, we employed the pole placement algorithm, then by designing proper polynomials gave it robust property, then due to a simple optimization routine, we make it fast and faster within the stability region. Finally, to evaluate the proposed method, numerical examples in different situations of the presence of noise, disturbance, and model uncertainties, also comparative results are presented. This paper proposed an accurate, fast, and robust controller. This can improve the performance of the perturbed functional systems used in the industrial fields. It is proposed to spread the benefit of fractional calculus in the control of complex systems in practical situations.

NOMENCLATURE AND SYMBOLS

q_n	Commensurate fractional order	PID	Proportional-Integral-Derivative
$E_{\alpha,\beta(z)}$	Mittag-Leffler function	VSC	Variable Structure Control
$\Gamma(.)$	Gamma function	SMC	Sliding-Mode Control
ζ	Time scale factor	SVSC	Soft Variable Structure Control
ζ_0	Maximum time scale factor	FPID	Fractional PID
α_k	characteristic ratios	CRA	Characteristic Ratio Assignment
$L\{.\}$	Laplace transform	PPC	Pole Placement Controller
FC	Fractional Calculus	TSMC	Terminal Sliding-Mode Control
FO	Fractional Order	FSMC	Fractional-order Sliding-Mode Control
FOS	Fractional-Order System	FO-PPC	Fractional Order Pole Placement Controller

I. Introduction

A. Background

The main goals of each control system are to achieve the appropriate speed and accuracy. Besides, the control systems demanded to be used in the industry suffer from degradation caused by model uncertainties and external disturbances. In this manuscript, with the benefit of recent findings on two wings Fractional Calculus (FC) and Variable Structure Control (VSC), we are to propose an accurate, fast, and robust controller. This can improve the performance of the perturbed functional systems; robust control provides a reliable base for future smart systems.

B. Literature review

As the first wing, in this work the FC is used to spread the benefit of FC in control of complex systems; moreover, the advantage of using FC in real application has been proven in recent research [1]. FC is the generalization of Integer-Order (IO) differentiation to Fractional-Order (FO) ones. It has a long history in mathematics, and today enhancing both transient and steady-state responses of the closed-loop performance is confirmed. Furthermore, FO controllers can make a very important role in robust systems against model uncertainties and disturbances [1, 2]. Fractional-order (FO) controllers offer greater flexibility in robustness that can only be achieved with high-order IO controllers [2]. Using FC in robust control can make a remarkable improvement compared to the conventional IO control [3]. In [4], an optimal approach for a fractional-order PID controller proposes to control electrical autonomous cars. In [5] the fractional-order PID controller in a combination of the type-2 fuzzy logic is developed for efficient and robust control of seismic systems. PID control as a common form of industrial control is faced limitations like uncertainties and parameter variations. Using FC in PID first proposed by Podlubny, and gives more efficiency in robustness of the system against gain variations [6, 7]. Sliding-Mode Control (SMC) as another traditional robust control strategy experiences chattering phenomenon, because of the switching non-linearity [8-10]. In [8], a model-free adaptive SMC is designed for control of input saturated chaotic systems. In [9] a fractional-order sliding mode controller is improved considering the estimated disturbance output. SMC uses a linear hyperplane as the sliding surface. In [10] a non-linear sliding mode observer is used to compensate cyber-attack and load disturbance in smart power systems. However, these control methods ensure asymptotic convergence of the system states to the equilibrium point, but there is no guarantee in finite-time. For a better robust control, the modified versions of SMC are used; like Higher-Order Sliding Mode Control, Terminal Sliding Mode Control (TSMC), etc... [11]. In [12] neural network-based TSMC is mentioned for control of the on-holonomic spherical robot. A deep recurrent neural networks with TSMC for a chaotic fractional-order financial system is proposed in [13]. Chattering is discussed still as a challenge in TSMC. Fuzzy and neural network approaches is used in SMC it's modified versions to enhance the robustness of systems [14]. In addition, using FC in SMC preserve all the advantages of SMC and additionally, can reduce chattering and to improve the robustness of the system. In [15] a new design of robust fractional adaptive decoupled control on a parallel micropositioning piezostage is proposed that contains three intuitional terms. A feedback model reference adaptive control term with fractional updating rules that represses the creep effect, external disturbances and parameters uncertainty, further increases the robustness and accuracy of positioning. However, this work assumes the prior knowledge of the upper bound of the system uncertainty. First use of fractional order control (FOC) in power electronics is mentioned in [16]. A new robust fractional-order super-twisting sliding mode control for supercapacitor-based power supply is proposed in [17]. As the chattering-free design of the controller, a robust, steady and smooth DC voltage can be provided. Also, this controller requires prior knowledge of the upper bound of system uncertainty.

On the second wing, VSC as an effective way to achieving the least settling time is performed. In VSC the control decision switches between n designed control way to achieve short settling times [18]. However, high frequency pattern switching in VSC is not desirable in industrial applications. So Soft Variable Structure Control (SVSC) introduced through increasing the number of predesigned structures to infinity in order to the selecting control function becomes continuous [18, 19]. But, because of the lack of robustness discussion, there is no reliability in the operational use of multitude of theatrical systems in the industrial environment.

C. Research gap and motivation

With an increasingly understanding of the potential of FOC, the number of studies and applications is increasing. However, by summarizing the current research results, it can be found that the research on this field is still at a preliminary stage. Our try is to develop a new control strategy for FO systems and help to complement the exploitation of the applications of FOS in modeling and controlling complex physical phenomena.

D. Challenges

To overcome the problem of disturbances in practice, applying FOC in variable structure schema is on the agenda; we are to solve the problems of modification of the RST control structure [19] with proper polynomials that guarantees the robustness of system, and propose a routine to vary the control signal continuously in a limited frame. The challenge relevant between velocity and parameters of the controller is adjusted by the Characteristic Ratio Assignment (CRA) method [20] in the FO pole placement algorithm [21]. The proposed VSC is to have a stable and robust control system,

with quick response, soft and restricted control signal.

E. Contribution

The contributions and novelties of the work are summarized as follows:

- The presented SVSC approach is raised in FO systems; compared with SVSC in [18] that are integer-order.
- The variable structure property of the proposed scheme, compared to fixed structure control in [22, 23], carries out a faster response, robust and stable control system, with a smooth and restricted control signal.
- In comparison with [19] that uses PSO, in this paper in order to decrease computational effort, a new simple and stable procedure for changing the parameters of the controller is proposed.
- In comparison with [19], system the robust performance and robust stability against external disturbances and model uncertainties is guaranteed.

F. Paper organization

This paper is organized as follows. In section 2 the procedure of the proposed SVSC is reviewed. Section 3 contains the stability and robustness discussion of the proposed control schema. Section 4 presents the simulations to validate the efficiency of the control system. Section 5 is dedicated to concluding remarks.

II. The proposed control scheme

To introduce the new proposed control scheme, we divided the dissection in four subsections: RST control structure, generalization to FO, desired commensurate system, and the SVSC approach.

A. RST control structure

The RST control structure is employed as a Pole Placement Controller (PPC) [20].

If we consider the system G and desired system G_m as follow:

$$G=\frac{B}{A}=\frac{b_n s^{q_n}+b_{n-1}s^{q_{n-1}}+\ldots+b_1 s^{q_1}+b_0}{a_m s^{p_m}+a_{m-1}s^{p_{m-1}}+\ldots+a_1 s^{p_1}+a_0} \quad (1)$$

$$G_m=\frac{B_m}{A_m}=\frac{b'_n s^{q'_n}+b'_{n-1}s^{q'_{n-1}}+\ldots+b'_1 s^{q'_1}+b'_0}{a'_m s^{p'_m}+a'_{m-1}s^{p'_{m-1}}+\ldots+a'_1 s^{p'_1}+a'_0} \quad (2)$$

Where $a_i, b_i, p_i, q_i \epsilon R$, $0<q_1<q_2<\cdots<q_n$ and $0<p_1<p_2<\cdots<p_m$. Also, $a'_i, b'_i, p'_i, q'_i \epsilon R$, $0<q'_1<q'_2<\cdots<q'_n$ and $0<p'_1<p'_2<\cdots<p'_m$. A_m is the desired characteristics polynomial and the A_c is closed loop characteristics polynomial from Diophantine equation:

$$AR+BS=A_c \quad (3)$$

So we will have:

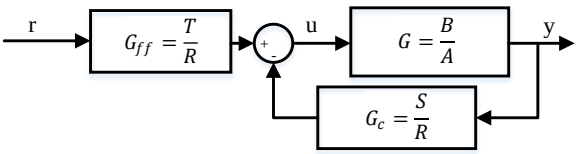

Fig 1. The RST control system

$$A_m y_{m(t)}=B_m u_{c(t)} \Rightarrow \frac{y_m}{u_c}=\frac{B_m}{A_m}=\frac{BT}{AR+BS}=\frac{BT}{A_C} \quad (4)$$

The controller polynomials R, S and T will be derived from (3) and (4).

B. Generalized FO-PPC

To generalize the RST method to FO-systems, at first, we make an integer-order reflection of FO polynomial. Therefore in polynomials, the minimum common resolution (q_n) will be chosen and substituted by δ. Second, the RST-based PPC will be applied to the reflective transfer functions [22].

$$G_{(\delta)}=\frac{B_{(\delta)}}{A_{(\delta)}}=\frac{b_n\delta^{p\beta_n}+b_{n-1}\delta^{p\beta_{n-1}}+\ldots+b_1\delta^{p\beta_1}+b_0}{a_m\delta^{p\alpha_m}+a_{m-1}\delta^{p\alpha_{m-1}}+a_1\delta^{p\alpha_1}+a_0} \quad (5)$$

$$G_{m(\delta)}=\frac{B_{m(\delta)}}{A_{m(\delta)}}=\frac{b'_n\delta^{gq'_n}+b'_{n-1}\delta^{gq'_{n-1}}+\ldots+b'_1\delta^{gq'_1}+b'_0}{a'_m\delta^{gp'_m}+a'_{m-1}\delta^{gp'_{m-1}}+a'_1\delta^{gp'_1}+a'_0} \quad (6)$$

The Diophantine equations (3 and 4) and Re-reflecting, give the S, R, and T, in FO form. By this design, the closed loop poles are directed to desired. Also, removing unstable zeros and poles is avoided.

C. Desired commensurate system

Because of the high-order nature of FOS, the velocity-parameters relation is adjusted by the CRA. According to CRA and Laplace scaling property, the response of closed loop systems (8), is ξ-times faster than the response systems (7) and the overshoots are the same.

$$G(s)=\frac{a_0}{a_n s^{qn}+a_{n-1}s^{q(n-1)}+\ldots+a_1 s^q+a_0} \quad (7)$$

$$G_{m(s)}=\frac{\zeta^{qn}a_0}{a_n s^{qn}+a_{n-1}\zeta^q s^{q(n-1)}+\ldots+\zeta^{q(n-1)}a_1 s^q+\zeta^{qn}a_0} \quad (8)$$

Where q is commensurate fractional order.

D. The SVSC approach

In the non-variable structure controller, the amplitudes of states decrease during the control period, so if we can modify the parameters of the controller during a control clock most capabilities of the control system can be used and earn a faster controller. Based on the proposed SVSC approach, at first, a FO-PPC will be designed; then the time-scaling factor ξ will be large and larger in the stability framework and constraint of the control signal. Changes in the controller's parameters make the system faster while the overall system is stable, the control signal is limited, and since the number of changes in the

controller decreases to infinity, the control signal is smooth.

In our proposed method, after shaping the FO-PPC, we try Increase ξ in $G_{m(s,\xi)}$ by consideration the following conditions:

$$\begin{aligned} &\xi_i > \xi_0 > 0 \\ &\left| r\frac{G_{ff}}{1-GG_c} \right| - |u_{max}| \le 0 \\ &|\xi_i - \xi_{i-1}| \le N\left|x_{(t)}\right| \end{aligned} \tag{9}$$

Where N is a positive constant. We have $\xi_i = \xi_{i-1} + Nx_{(t)}$ and if the condition (9) is not fulfilled in the increase ξ, then $\xi_i = \xi_{i-1} - s_D x_{(t)}$ until establishment of (9). s_D is a positive constant. So we get the biggest time-scaling factor ξ, the desired commensurate system will be reshape in each control period i , and by applying the controller the overall system were faster and faster.

III. Stability, sensitivity and robustness

In this section, the stability discussion of the system is provided in subsections on internal and overall time-variant system stability. Also, the sensitivity and robustness of the proposed system against external disturbances, noise, and model uncertainties is interpreted.

A. Internal stability

In order to have internal stability and model following condition, BT and A_c have to have no common factor in in Diophantine equations (3, 4). So we separate polynomial B into B^+ and B^- as stable and an unstable part (10). The unstable poles of B^- cannot be canceled and it can cause instability problem; to overcome this problem, we can consider B^-as a part of B_m (11). And, B^+ should be a common factor in A_c and R (12, 13).

$$B = B^- B^+ \tag{10}$$

$$B_m = B^- B'_m \tag{11}$$

$$R = R'B^+ \tag{12}$$

$$A_c = A_0 . A_m . B^+ \tag{13}$$

Where A_0 is the residual part poles. Therefore, the Diophantine equation is reduced as bellows.

$$AR' + B^- S = A_0 A_m \tag{14}$$

Also, about T we will have

$$T = A_0 B'_m \tag{15}.$$

B. Time-variant system stability

Changing the controller parameters during every control clock leads the proposed controller to a FO time-variant system. We consider the proposed SVSC as the following system.

$$\frac{d^{\alpha}}{dt^{\alpha}} x(t) = \tilde{A}(t)x(t) = \bar{A}x(t) + \Delta A(t)x(t) \tag{16}$$

Where $x(t) \in R^n$ is the system state vector, $\tilde{A}(t) \in R^{n\times n}$ is system equivalent matrix. The VSC approach produces the time-variant portion , $\Delta A(t) \in R^{n\times n}$, the , $\bar{A}(t) \in R^{n\times n}$ is a constant matrix, and $0 < \alpha < 2$ is fractional order

In the following, before presenting the main theory of stability of the studied system, it is necessary to mention some definitions and lemmas.

Definition 1: The α-order Caputo derivative of function $h_{(t)}$ is defined as (17), and its Laplace transform at $t_0 = 0$ is written as (19) [1].

$${}_{t_0}^{C}D_t^{\alpha} h(t) = \frac{1}{\Gamma(n-\alpha)} \int_{t_0}^{t} (t-\tau)^{n-\alpha-1} h^{(n)}(\tau) d\tau, \quad n-1 < \alpha \le n \tag{17}$$

$$\Gamma(\tau) = \int_0^{\infty} t^{\tau-1} e^{-t} dt. \tag{18}$$

$$\int_0^{\infty} e^{-st} {}_{t_0}^{C}D_t^{\alpha} x(t) dt = s^{\alpha} X(s) - \sum_{k=0}^{n-1} s^{\alpha-k-1} x^{(k)}(0), (n-1 < \alpha \le n) \tag{19}$$

Where $\Gamma(.)$ denotes the Gamma function.

Definition 2: The system ${}_{t_0}^{C}D_t^{\alpha} x(t) = g_{(t,x(t))}$, $0 < \alpha \le 1$ (also $1 < \alpha < 2$) is stable if, for any initial values, there is $\varepsilon > 0$ such that $\|x\| < \varepsilon$ for all $t > t_0$. The system is asymptotically stable if $\|x\| \to 0$ as $t \to +\infty$.

Definition 3 [1, 24]: The introduction of Mittag-Leffler function is mentioned in (20), and its two-parameters form and its Laplace transform are mentioned in (21) and (22).

$$E_{\alpha}(z) = \sum_{k=0}^{\infty} \frac{z^k}{\Gamma(k\alpha + 1)} \tag{20}$$

$$E_{\alpha,\beta}(z) = \sum_{k=0}^{\infty} \frac{z^k}{\Gamma(k\alpha + \beta)} \tag{21}$$

$$L\left\{ t^{\beta-1} E_{\alpha,\beta}(-\lambda t^{\alpha}) \right\} = \frac{s^{\alpha-\beta}}{s^{\alpha} + \lambda}, (R(s) > |\lambda|^{\frac{1}{\alpha}}) \tag{22}$$

Where z is a complex number, $0 < \alpha$, $0 < \beta$ and $L\{.\}$, is the Laplace transform symbol. In particular, if $\alpha = 1$ and $\beta = 1$, then $E_{1,1}(z) = e^z$.

Lemma 1 [19]: If $A \in C^{n\times n}$ and $0 < \alpha < 2$, μ satisfies $\pi\alpha/2 < \mu < \min\{\pi, \pi\alpha\}$, β is an arbitrary real number, and $P > 0$ is a real constant, then Mittag-Leffler function in (23) applies.

$$\left\|E_{\alpha,\beta}(A)\right\| \le \frac{\mathrm{P}}{1+\|A\|} \tag{23}$$

In which $\mu \le \left|\arg(spec(A))\right| \le \pi$, $\|.\|$ is the L_2 norm and $spec(.)$ denotes the eigenvalues of the matrix.

Lemma 2: based on Gronwall inequality [19] for all continuous functions on $[t_0,T), T \le +\infty$, $k(t) \ge 0$ and we have

$$x(t) \le h(t) + \int_{t_0}^{t} k(s)x(s)ds, \qquad t \in [t_0,T) \tag{24}$$

then $x(t)$ convinces

$$x(t) \le h(t) + \int_{t_0}^{t} k(s)h(s)\exp\left[\int_{s}^{t} k(u)du\right]ds. \tag{25}$$

Theorem 1: For *fractional order* α if*:*

a) $0 < \alpha \le 1$, $\left|\arg(spec(A))\right| > \alpha\pi/2$, $\alpha\|A\| > 1$, *and* $\Delta A(t)x(t)$ *in* $\lim_{x\to 0} {}^{\|\Delta A(t)x(t)\|}/_{\|x(t)\|} = 0$ *applies,*

b) $1 < \alpha \le 2$, $\left|\arg(spec(A))\right| > \alpha\pi/2$, $(\alpha-1)\|A\| > 1$, *and* $\Delta A(t)x(t)$ *in* $\lim_{x\to 0} {}^{\|\Delta A(t)x(t)\|}/_{\|x(t)\|} = 0$ *applies,*

then the system (16) is asymptotically stabile.

Proof. (a). The PPC system is as follows.

$$D^{\alpha}X = AX + Bu = (A+BK)X = \bar{A}X \tag{26}$$

Where $K \in R^n$ includes the pole placement gains and $A + BK = \bar{A}$. So the time-variant proposed SVSC can be considered as (16).

To get the solution of (16), firstly we take Laplace transform on (16), and secondly Laplace inverse transform.

$$X(s) = (Is^{\alpha} - A)^{-1}(s^{\alpha-1}x_0 + L\{\Delta A(t)x(t)\}) \tag{27}$$

$$x(t) = E_{\alpha,1}(A(t-t_0)^{\alpha})x_0 + \int_{t_0}^{t}((t-\tau)^{\alpha-1}E_{\alpha,\alpha}(A(t-\tau)^{\alpha})\Delta A(\tau)x(\tau)d\tau, \tag{28}$$

Where I is identity matrix.

Lemma 1 says that there exist positive constants P and P_0 that get as follows.

$$\|x(t)\| \le \frac{\mathrm{P}\|x_0\|}{1+\|A\|(t-t_0)^{\alpha}} + \int_{t_0}^{t}\frac{(t-\tau)^{\alpha-1}\mathrm{P}_0}{1+\|A\|(t-\tau)^{\alpha}}\|\Delta A(\tau)x(\tau)\|d\tau \tag{29}$$

Considering the assumption $|\xi_i - \xi_{i-1}| \le N|x_{(t)}|$ we have

$$\|\Delta A(t)x(t)\| \le \frac{1}{\mathrm{P}_0}\|x(t)\| \tag{30}$$

Substituting (30) into (29), we gets

$$\|x(t)\| \le \frac{\mathrm{P}\|x_0\|}{1+\|A\|(t-t_0)^{\alpha}} + \int_{t_0}^{t}\frac{(t-\tau)^{\alpha-1}}{1+\|A\|(t-\tau)^{\alpha}}\|x_{(\tau)}\|d\tau \quad ,(31)$$

By applying Lemma 2 on (31), results in:

$$\|x(t)\| \le \frac{\mathrm{P}\|x_0\|}{1+\|A\|(t-t_0)^{\alpha}} + \mathrm{P}\int_{t_0}^{t}\frac{(t-\tau)^{\alpha-1}\|x_0\|}{(1+\|A\|(\tau-t_0)^{\alpha}(1+\|A\|(t-\tau)^{\alpha})}\times \exp\left(\int_{\tau}^{s}\frac{(t-s)^{\alpha-1}ds}{(1+\|A\|(t-s)^{\alpha}}\right)d\tau = \frac{\mathrm{P}\|x_0\|}{1+\|A\|(t-t_0)^{\alpha}} + \mathrm{P}\int_{t_0}^{t}\frac{(t-\tau)^{\alpha-1}\|x_0\|}{(1+\|A\|(\tau-t_0)^{\alpha})(1+\|A\|(t-\tau)^{\alpha})\left(1-\frac{1}{\alpha\|A\|}\right)} \le \frac{P\|x_0\|}{1+\|A\|(t-t_0)^{\alpha}} + \mathrm{P}\|x_0\|\|A\|^{\left(\frac{1}{\alpha\|A\|}-2\right)}\int_{t_0}^{t}(t-\tau)^{\frac{1}{\|A\|}-1}(\tau - t_0)^{-\alpha}d\tau = \frac{P\|x_0\|}{1+\|A\|(t-t_0)^{\alpha}} + \mathrm{P}\|x_0\|\|A\|^{\left(\frac{1}{\alpha\|A\|}-2\right)}\frac{\Gamma\left(\frac{1}{\|A\|}\right)\Gamma(1-\alpha)}{\Gamma\left(1+\frac{1}{\|A\|}-\alpha\right)}(t - t_0)^{\frac{1}{\|A\|}-\alpha} \tag{32}$$

Thus, when $t \to +\infty, \|x(t)\| \to 0$ for $\alpha\|A\| > 1$, that ensures the asymptotic stability of the system (16).

(b) assume $x^{(k)}(t_0) = x_k (k = 0,1)$ as initial conditions. Through the Laplace and Laplace inverse transform, the output of (16) is as follows.

$$x(t) = E_{\alpha,1}(A(t-t_0)^{\alpha})x_0 + (t-t_0)E_{\alpha,2}(A(t-t_0)^{\alpha})x_1 + \int_{t_0}^{t}(t-\tau)^{\alpha-1}E_{\alpha,\alpha}(A(t-\tau)^{\alpha})\Delta A(\tau)x(\tau))d\tau. \tag{33}$$

Lemma 1 says that there exist positive constants P_1, P_2, and P_3 such that

$$\|x(t)\| \le \frac{\mathrm{P}_1\|x_0\|}{1+\|A\|(t-t_0)^{\alpha}} + \frac{\mathrm{P}_2(t-t_0)\|x_1\|}{1+\|A\|(t-t_0)^{\alpha}} + \int_{t_0}^{t}\frac{\mathrm{P}_3(t-\tau)^{\alpha-1}}{1+\|A\|(t-\tau)^{\alpha}}\|\Delta A(\tau)x(\tau)\|d\tau \tag{34}$$

Considering the assumption $|\xi_i - \xi_{i-1}| \le N|x_{(t)}|$ we have

$$\|\Delta A(t)x(t)\| \le \frac{1}{\mathrm{P}_3}\|x(t)\| \tag{35}$$

Submitting (35) into (34), we gets

$$\|x(t)\| \le \frac{\mathrm{P}_1\|x_0\| + \mathrm{P}_2(t-t_0)\|x_1\|}{1+\|A\|(t-t_0)^{\alpha}} + \int_{t_0}^{t}\frac{(t-\tau)^{\alpha-1}}{1+\|A\|(t-\tau)^{\alpha}}\|\Delta A(\tau)x(\tau)\|d\tau \tag{36}$$

By applying Lemma 2 on (36), results in:

$$\|x(t)\| \le \frac{\mathrm{P}_1\|x_0\|+\mathrm{P}_2(t-t_0)\|x_1\|}{1+\|A\|(t-t_0)^{\alpha}} + \int_{t_0}^{t}\frac{(\mathrm{P}_1\|x_0\|+\mathrm{P}_2(t-t_0)\|x_1\|)(t-\tau)^{\alpha-1}}{(1+\|A\|(\tau-t_0)^{\alpha}(1+\|A\|(t-\tau)^{\alpha})}\times \exp\left(\int_{\tau}^{s}\frac{(t-s)^{\alpha-1}ds}{(1+\|A\|(t-s)^{\alpha}}\right)d\tau = \frac{\mathrm{P}_1\|x_0\|+\mathrm{P}_2(t-t_0)\|x_1\|}{1+\|A\|(t-t_0)^{\alpha}} + \int_{t_0}^{t}\frac{(\mathrm{P}_1\|x_0\|+\mathrm{P}_2(t-t_0)\|x_1\|)(t-\tau)^{\alpha-1}}{(1+\|A\|(\tau-t_0)^{\alpha})(1+\|A\|(t-\tau)^{\alpha})\left(1-\frac{1}{\alpha\|A\|}\right)} \le \frac{\mathrm{P}_1\|x_0\|+\mathrm{P}_2(t-t_0)\|x_1\|}{1+\|A\|(t-t_0)^{\alpha}} + \mathrm{P}_1\|x_0\|\|A\|^{\left(\frac{1}{\alpha\|A\|}-2\right)}\frac{\Gamma\left(\frac{1}{\|A\|}\right)\Gamma(1-\alpha)}{\Gamma\left(1+\frac{1}{\|A\|}-\alpha\right)}(t - t_0)^{\frac{1}{\|A\|}-\alpha} + \mathrm{P}_2\|x_1\|\|A\|^{\left(\frac{1}{\alpha\|A\|}-2\right)}\frac{\Gamma\left(\frac{1}{\|A\|}\right)\Gamma(2-\alpha)}{\Gamma\left(2+\frac{1}{\|A\|}-\alpha\right)}(t - t_0)^{\frac{1}{\|A\|}-\alpha} \tag{37}$$

Therefore, if $(\alpha-1)\|A\| > 1$, then $\|x(t)\| \to 0$ as $t \to +\infty$, which implies that the system (16) is asymptotically stable.

C. External disturbances

Assume that there is a process disturbance d and measurement noise n as is illustrated in Fig. 2. In the system in Fig. 2 y is the process output and y_n denotes the measured signal. So for the signals y, y_n, and u we have:

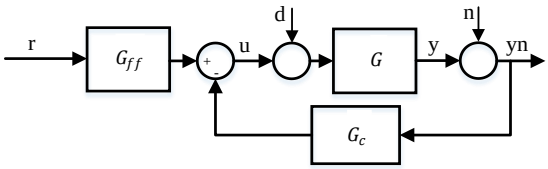

Fig 2. Block diagram of closed-loop system with load disturbance d and measurement noise n

$$\begin{aligned} Ay &= B(u+d) \\ y_n &= y + n \\ Ru &= Tr - Sy_n \end{aligned} \tag{38}$$

$$\begin{aligned} y &= \frac{BT}{AR+BS}r + \frac{BR}{AR+BS}d + \frac{BS}{AR+BS}n \\ y_n &= \frac{BT}{AR+BS}r + \frac{BR}{AR+BS}d + \frac{AR}{AR+BS}n \\ u &= \frac{AT}{AR+BS}r - \frac{BS}{AR+BS}d - \frac{AS}{AR+BS}n \end{aligned} \tag{39}$$

These equations show the effect of command signals and disturbances in the closed-loop system response separately. The design of the closed-loop system assumed always stable, so all the roots of characteristic polynomial $A_c = AR + BS$ is in the left half plane. The Diophantine algebraic problem is finding two polynomials $R_{(s)}$ and $S_{(s)}$ for given $A_{(s)}$, $B_{(s)}$, and $A_{c(s)}$ from one equation (3). The designer can consider the auxiliary constraints by choosing an appropriate polynomial and obtaining another one.

First, consider the low frequency load disturbance d is a step. To avoid that there is a steady-state error we must require that the static gain from the disturbance d to y_n is zero. This means that $\lim_{s\to 0} B_{(s)} R_{(s)} = 0$. If the process itself has a nonzero gain, s must be a factor of $R(s)$. Secondly, measurement noise is typically of high frequency. One way to make sure that measurement noise does not generate large signals is to require that the controller G_c have a low-pass filter nature. This means that measurement signals do not give any errors in the process variable. To summarize, the disturbances can be dealt with by introducing constraints on the polynomials R and S.

D. Model uncertainties

If we consider that the design of the controller is based on the nominal uncertain model$G$, true open-loop transfer function is $\hat{G}$; The closed-loop system will be T_{cl} and $\hat{T}_{cl}$ respectively.

$$T_{cl} = \frac{G_{ff}G}{1 + G_c G} \tag{40}$$

$$\hat{T}_{cl} = \frac{G_{ff}\hat{G}}{1 + G_c \hat{G}} \tag{41}$$

The sensitivity of closed-loop system respect to variations in G is given by

$$\frac{dT_{cl}}{dG} = \frac{G_{ff}}{(1 + G_c G)^2} \tag{42}$$

The relative sensitivity of closed-loop system respect to G can be written as

$$\frac{dT_{cl}}{T_{cl}} = \frac{1}{1 + G_c G}\frac{dG}{G} = \Gamma\frac{dG}{G} \tag{43}$$

The transfer function Γ is called sensitivity function and transfer function Δ is called complementary sensitivity.

$$\Gamma = \frac{1}{1 + G_c G} \tag{44}$$

$$\Delta = 1 - \Gamma = \frac{G_c G}{1 + G_c G} \tag{45}$$

The poles of the closed-loop system are the zeros of the function

$$\begin{aligned} f_{(s)} &= 1 + G_{c(s)}\hat{G}_{(s)} \\ &= 1 + G_{c(s)}\hat{G}_{(s)} + G_{c(s)}G_{(s)} - G_{c(s)}G_{(s)} \\ &= 1 + G_{c(s)}G_{(s)} + G_{c(s)}(\hat{G}_{(s)} - G_{(s)}) \end{aligned} \tag{46}$$

If in the left half plane

$$\left|G_{c(s)}(\hat{G}_{(s)} - G_{(s)})\right| \le |\,1 + G_c G| = \left|\frac{G}{T_{cl}}\right| |G_{ff}| \tag{47}$$

Then it follows from the principle of variation of the argument that the differences between the number of poles and zeros in right half plane for the function $1 + G_c G$ and $1 + G_c \hat{G}$ are the same. The relative precision needed for stability robustness is obtained by dividing by $G_c G$.

$$\left|\frac{\hat{G} - G}{G}\right| \le \left|\frac{1 + G_c\hat{G}}{G_c G}\right| = \left|\frac{1}{\Delta}\right| \tag{48}$$

The complementary sensitive function thus makes it possible to determine bounds for stability robustness. The following theorem results.

Theorem 2: Consider the closed-loop systems T_{cl} and $\hat{T}_{cl}$ obtained from systems with transfer functions G and $\hat{G}$ I respectively. The system $\hat{T}_{cl}$ is stable if the following conditions are true:

1. T_{cl} is stable.

2. G and $\hat{G}$ have the same number of poles in right half plane.
3. The inequality (47) is fulfilled in left half plane.

The result shows that the designer must know the number of unstable modes in order to design a regulator for the system. The theorem is, however, conservative. The inequality (47) gives the frequency range in which it is important to have a good description of the process where $\hat{G}_{(s)} \approx 1$.

The transfer function of the closed-loop system given in (41) can also be written as bellows.

$$T_{cl} = \frac{1}{1 + {}^{1}/_{G_c \hat{G}}} \tag{49}$$

The poles of the closed-loop system are thus the zeros of the function.

$$\begin{aligned} f_{(s)} &= 1 + \frac{1}{G_{c(s)}\hat{G}_{(s)}} \\ &= 1 + \frac{1}{G_{c(s)}\hat{G}_{(s)}} + \frac{1}{G_{c(s)}G_{(s)}} - \frac{1}{G_{c(s)}G_{(s)}} \end{aligned} \tag{50}$$

It follows from the principle of variation of the argument that the differences between the zeros and poles in right half plane of the functions $1 + \frac{1}{G_{c(s)}\hat{G}_{(s)}}$ and $1 + \frac{1}{G_{c(s)}G_{(s)}}$ are the same if in the left half plane

$$\left| \frac{1}{G_{c(s)}\hat{G}_{(s)}} - \frac{1}{G_{c(s)}G_{(s)}} \right| < \left| 1 + \frac{1}{G_{c(s)}G_{(s)}} \right| \tag{51}$$

Theorem 3: Consider the closed-loop systems T_{cl} and $\hat{T}_{cl}$ obtained from transfer functions G and $\hat{G}$ respectively. The system $\hat{T}_{cl}$ is stable if the following conditions are true:

1. T_{cl} is stable.
2. G and $\hat{G}$ have the same number of zeros in right half plane.
3. The inequality (51) is fulfilled on the Im axe of complex plane.

The theorem shows that stability can be maintained in spite of large differences between G and Gˆ provided that the loop gain is large.

Based on theorems 2 and 3, to achieve robust stability based on an uncertain model the following rules are obtained.

- The designer must know the number of unstable poles and zeros.
- The designer must know the model precisely for those frequencies for which the loop gain can be made large.
- The designer must make the loop gain small for those frequencies for which the relative error $\frac{\Delta G}{G}$ is large.
- The designer must have a model that describes the system precisely for those frequencies for which $\hat{G} \approx -1$

IV. Simulation tests

The DC/DC converters that convert an unregulated input voltage to a regulated output voltage have an important role in energy storage systems to increase the efficiency of power conversion [25]. In recent studies, modeling of DC/DC converters in FO systems has been considered by many researchers. The following sample model is used for numerical example simulations on FO DC/DC buck converter [26] to show the efficiency of proposed method.

$$G_{(s)} = \frac{V_o}{D} = \frac{V_i}{L_\alpha C_\beta s^{\alpha+\beta} + \frac{L_\alpha}{R} s^{\alpha} + 1} \tag{52}$$

Where and α and β reflect the non-ideality of inductor and capacitor model and L_α and C_β is fractional order inductance and capacitance. The control signal D is input duty-cycle, V_o is output voltage and V_i is input voltage. The parameters considered as L=4.7 mH, C=10 mF, R=5 Ω, α=0.9, β=0.8 and V_i=1 V. Taking into account the desired response characteristics and the given actuator constraint $|D_{max}| = 1$ the desired system is assumed as follows.

$$G_{m(s.\zeta)} = \frac{1024\zeta^2}{s^2 + 64\zeta s + 1024\zeta^2} \tag{53}$$

Through this G_m, by $\zeta_0 = 1$ the fastest possible system regarding actuator constraint will be obtained.

A. The simulation structure

In the simulation structure Fig. 3, the controller is performed as a function, by selecting polynomial $S_{(s)} = {}^{1}/_{s + \frac{V_i}{1024\xi^2}}$ and solving Diophantine equation (3), the controller's polynomials will be obtained as (54) and (55).

$$\begin{aligned} R &= \frac{1024\xi^2 s^3 + (65536\xi^3 + L_\alpha C_\beta V_i)s^2 + (1024^2\xi^4 + 64V_i\xi)s}{L_\alpha C_\beta 1024\xi^2 s^{2.7} + \frac{L_\alpha}{R}1024\xi^2 s^{1.9} + L_\alpha C_\beta V_i s^{1.7} + \frac{L_\alpha}{R}V_i s^{0.9} + 1024\xi^2 s + V_i} \\ &\quad (54) \end{aligned}$$

$$T = \frac{1024\xi^2}{V_i} \tag{55}$$

In performing SVSC schema, we got N=10 and decreasing step $s_D = 0.05$. By this design we have s-factor in the $R(s)$ cause to disappear low frequency step disturbance in steady-state, also, the controller G_c have low-pass filter nature, so it

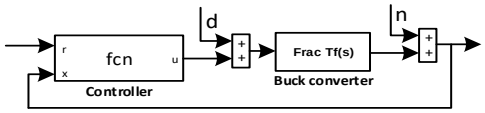

Fig 3. The simulation structure

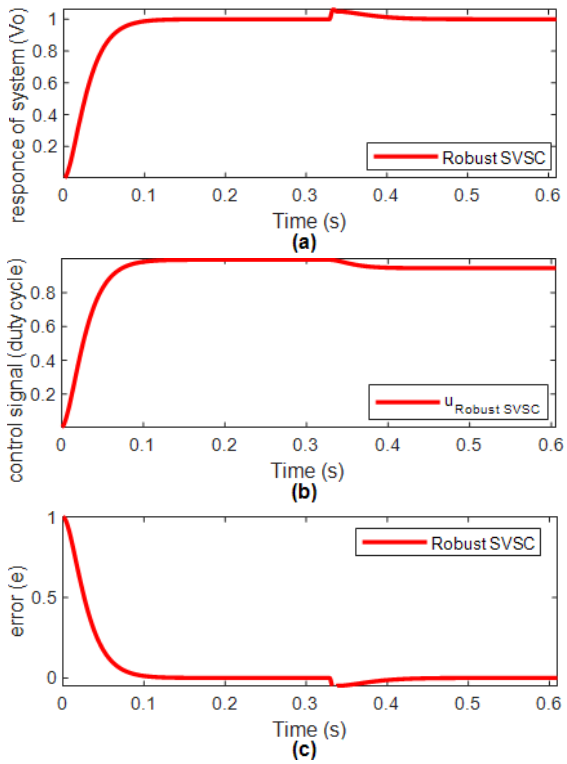

Fig 4. Output (a), control signal (b) and error (c) of the proposed controller in the presence of disturbance.

can eliminate the high frequency noise. Furthermore, by considering conditions in Theorem 2 and Theorem 3, the closed-loop system in the presence of model uncertainty will stay stable.

B. The simulation tests

a) In the presence of disturbance

In order to evaluate the controller in the presence of disturbance, the control system is affected by step load disturbance with amplitude $0.05|D_{max}| = 0.05$ in t=0.35s is shown in Fig. 4.

As a physical interpretation of Fig. 4, the disturbance deviation in the duty cycle is well compensated. It is illustrated that the control system has eliminated the effect of disturbance within an acceptable period of time and the control signal behaves smoothly within the actuator constraint range.

b) In the presence of model uncertainties

In this simulation case, the parameter of system $G_{(s)}$ is replaced by the values $a2 = 0.8a2$, $a1 = 0.82a1$, $and\ a0 = 0.78a0$ in time 0.35s. From a physical point of view, this case can be interpreted as changes in the value of electrical elements due to wear or environmental conditions.

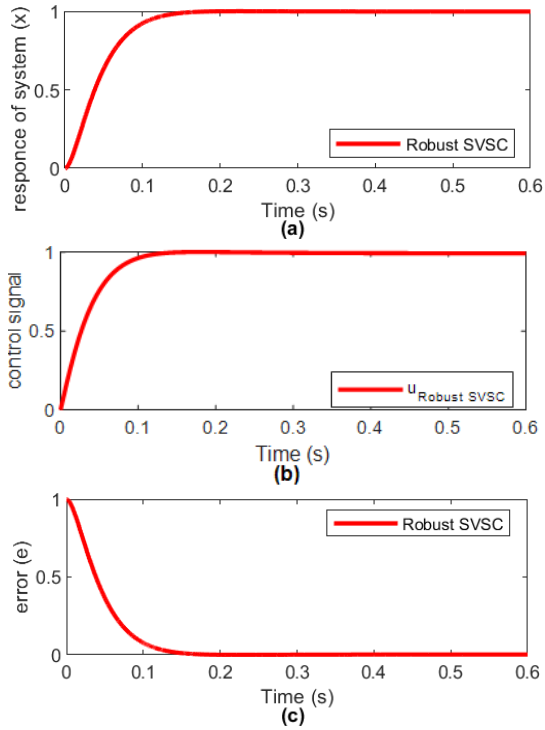

Fig 5. Output (a), control signal (b) and error (c) of the proposed controller in the presence of model uncertainty.

As is illustrated in Fig. 5, the controller has an acceptable performance in the presence of significant model uncertainty. There is no considerable effect on response and control signal of the system.

c) In the presence of noise, disturbance and model uncertainties

In the following case, In addition to disturbance and model uncertainties, the response signal is corrupted by measurement noise. The 29dB white Gaussian noise is added to measured signal, step load disturbance with amplitude 0.05 in t=0.35s and the parameter change as case b is forced to system. Fig. 5 shows the performance of the controller in this environment.

As can be seen, the performance in the presence of noise, disturbance and model uncertainties is satisfactory. The control system can tolerate the noise, disturbance and model uncertainties. There is no change in the settling time, and the control signal is smooth within the actuator constraint range.

d) Comparative results

To improve the results and discussions, a comparison with methods Fractional-order Sliding-Mode Control [27] and Fractional-order PID (FPID) [28] is presented. For these cases the fractional sliding surface is selected as follows:

$$S = e^{(0.7)} + \lambda e, \tag{56}$$

Where λ=1; and parameters of the FPID selected thorough MATLAB SQP_ ITSE optimization ($P = 0.10,\ I = 22.08$

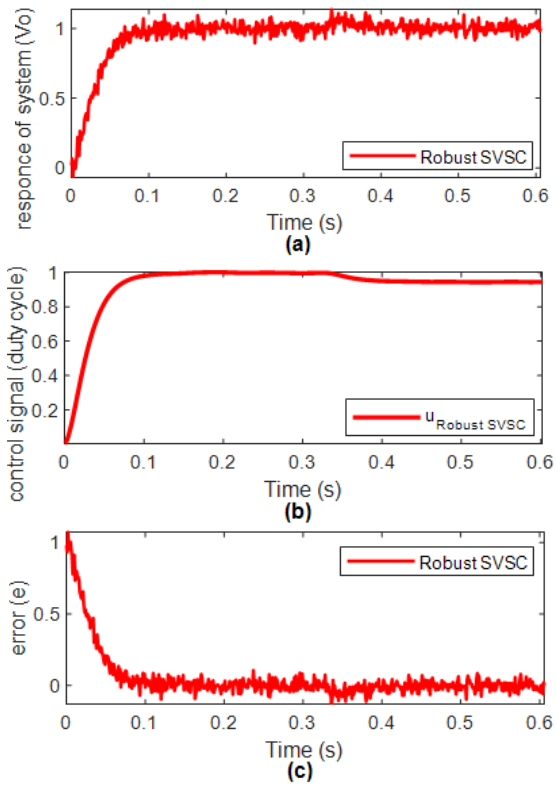

Fig 6. Output (a), control signal (b) and error (c) of the proposed controller in the presence of disturbance, model uncertainty and noise

Table 1.Table of results

method	t_s	$\mathbf{u_{max}}$
Robust SVSC	0.15s	1.0 (by restriction)
FSMC	0.24s	1.0
FPID	0.41s	1.0

$\lambda = 0.78,\ D = 0.02,\ and\ \mu = 0.09$). Fig. 6 shows the comparative performance of the controllers. Table 1 summarizes the simulation results.

As is illustrated, the SMC is as fast as the proposed controller, and has good robustness against uncertainties; but the SMC is diagnosed with chattering, while the control signal of the proposed controller is smooth. Plus, there is no restriction barrier on the control signal in FSMC and FPID. By the initiative presented in this article, during the control period it exploits the maximum capacity of the actuator; and by selecting proper polynomials in controller design, the robust performance and robust stability against external disturbances and model uncertainties was obtained. Therefore, we could implement a faster controller while considering control signal constraints in the presence of model uncertainties and external disturbances. The control signal is soft and has no chattering.

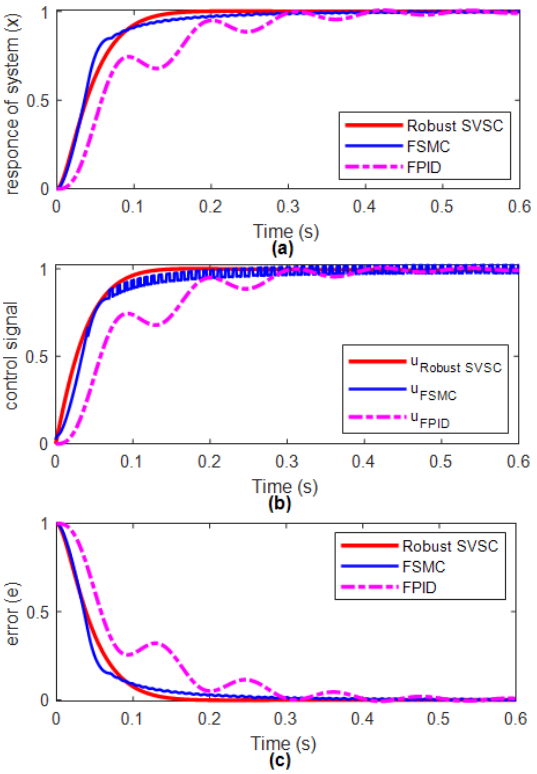

Fig 7. Comparison of the proposed controller with FSMC and FPID: response (a), the control signal (b), and error (c)

V. Conclusions

In this paper, the fractional-order floated pole controller as a fast and robust approach for the FO systems is proposed. The proposed robust variable structure control yields a continuous and constrained control signal, also a fast response in the presence of model uncertainties and external disturbances. In the proposed method, the pole placement algorithm is employed, the robust property added to the controller by designing proper polynomials, then due to a simple optimization routine it made fast and faster within the stability region. In the proposed robust system, a continuous and constrained control signal is get. The sufficient condition of stability is developed based on attributes of the Mittag-Leffler function and the stability theory of FOS. Numerical simulations and examples are done to demonstrate the effectiveness of the proposed method. As the future scope, the generalization of other SVSC methods to FO systems can be relevant. Also as a recommendation for the practical use of the proposed method in real life, the Oustaloup approximation and Hankel model order reduction techniques can be used for approximation to integer order systems and reduce the complexity of such high-order integer controllers, respectively.

References

[1] P. Warrier and P. Shah, "Fractional Order Control of Power Electronic Converters in Industrial Drives and Renewable Energy Systems: A Review," in IEEE Access, vol. 9, pp. 58982-59009, 2021, doi: 10.1109/ACCESS.2021.3073033.

[٢] Gholipour, R., Fateh, M.M. Robust Control of Robotic Manipulators in the Task-Space Using an Adaptive Observer Based on Chebyshev Polynomials. J Syst Sci Complex 33, 1360–1382 (2020). https://doi.org/10.1007/s11424-020-8186-0

[٣] Y. Chen, I. Petras, and D. Xue, ''Fractional order control—A tutorial,'' in Proc. Amer. Control Conf., Jun. 2009, pp. 1397–1411.

[٤] Batiha IM, Ababneh OY, Al-Nana AA, Alshanti WG, Alshorm S, Momani S. A Numerical Implementation of Fractional-Order PID Controllers for Autonomous Vehicles. Axioms. 2023 Mar 17;12(3):306.

[٥] Zamani AA, Etedali S. Seismic structural control using magneto-rheological dampers: A decentralized interval type-2 fractional-order fuzzy PID controller optimized based on energy concepts. ISA transactions. 2023 Feb 7.

[٦] S. Pandey, P. Dwivedi, and A. S. Junghare, ''A novel 2-DOF fractional-order PI λ – D μ controller with inherent anti-windup capability for a magnetic levitation system,'' AEU-Int. J. Electron. Commun., vol. 79, pp. 158–171, Sep. 2017.http://www.sciencedirect.com/science/article/pii/S1434841117301905

[7] P. Shah and S. Agashe, ''Review of fractional PID controller,'' Mechatronics, vol. 38, pp. 29–41, Sep. 2016. http://www.sciencedirect.com/science/article/pii/S095741581630068X

[8] Chen Y, Tang C, Roohi M. Design of a model-free adaptive sliding mode control to synchronize chaotic fractional-order systems with input saturation: An application in secure communications. Journal of the Franklin Institute. 2021 Oct 1;358(16):8109-37.

[9] Mohammad Ghamgosar, Seyed Mehdi Mirhosseini-Alizamini, Mahmood Dadkhah, Design of Optimal Sliding Mode Control based on Linear Matrix Inequality for Fractional Time-Varying Delay Systems, International Journal of Industrial Electronics, Control and Optimization (IECO), Volume 5, Issue 4 , December 2022, , Pages 317-325, https://doi.org/10.22111/ieco.2022.42132.1423 ..

[10] Rouhani SH, Mojallali H, Baghramian A. Load frequency control in the presence of simultaneous cyber-attack and participation of demand response program. Transactions of the Institute of Measurement and Control. 2022 Jun;44(10):1993-2011.

[11] Shokoohinia, M.R., Fateh, M.M. & Gholipour, R. Design of an adaptive dynamic sliding mode control approach for robotic systems via uncertainty estimators with exponential convergence rate. SN Appl. Sci. 2, 180 (2020). https://doi.org/10.1007/s42452-020-1947-5.

[12] Chen SB, Beigi A, Yousefpour A, Rajaee F, Jahanshahi H, Bekiros S, Martínez RA, Chu Y. Recurrent neural network-based robust nonsingular sliding mode control with input saturation for a non-holonomic spherical robot. IEEE access. 2020 Oct 13;8:188441-53.

[13] Wang YL, Jahanshahi H, Bekiros S, Bezzina F, Chu YM, Aly AA. Deep recurrent neural networks with finite-time terminal sliding mode control for a chaotic fractional-order financial system with market confidence. Chaos, Solitons & Fractals. 2021 May 1;146:110881.

[14] Dipayan Guha, Provas Kumar Roy, Subrata Banerjee, Adaptive fractional-order sliding-mode disturbance observer-based robust theoretical frequency controller applied to hybrid wind–diesel power system, ISA Transactions, 2022, ISSN 0019-0578, https://doi.org/10.1016/j.isatra.2022.06.030.

[15] S. Hou, Y. Chu, and J. Fei, ''Intelligent global sliding mode control using recurrent feature selection neural network for active power filter,'' IEEE Trans. Ind. Electron., early access, Jun. 12, 2020, doi: 10.1109/TIE.2020.3000098.

[16] J. Wang, W. Luo, J. Liu, and L. Wu, ''Adaptive type-2 FNN-based dynamic sliding mode control of DC–DC boost converters,'' IEEE Trans. Syst., Man, Cybern. Syst., vol. 51, no. 4, pp. 2246–2257, Apr. 2021.

[17] Shengzheng Kang, Hongtao Wu, Xiaolong Yang, Yao Li, Liang Pan, Bai Chen, Fractional robust adaptive decoupled control for attenuating creep, hysteresis and cross coupling in a parallel piezostage, Mechanical Systems and Signal Processing, Volume 159, 2021, 107764,ISSN 0888-3270, https://doi.org/10.1016/j.ymssp.2021.107764.

[18] Kaheni M, Zarif MH, Kalat AA, Fadali MS. Soft variable structure control of linear systems via desired pole paths. Information Technology and Control/Informacinės technologijos ir valdymas. 2018 Sep 10;47(3):447-56.

[19] Abbaszadeh E, Haddad-Zarif M. Soft variable structure control of linear fractional-order systems with actuators saturation. ISA transactions. 2022 Mar 10.

[20] Åström KJ, Wittenmark B. Computer-controlled systems: theory and design. Courier Corporation; 2013 Jun 13.

[21] Tabatabaei M, Haeri M. Characteristic ratio assignment in fractional order systems. ISA transactions. 2010 Oct 1;49(4):470-8.

[22]Rasouli H, Fatehi A, Zamanian H. Design and implementation of fractional order pole placement controller to control the magnetic flux in Damavand tokamak. Review of Scientific Instruments. 2015 Mar 10;86(3):033503.

[23] Junior FA, Bessa I, Pereira VM, da Silva Farias NJ, de Menezes AR, de Medeiros RL, Chaves Filho JE, Lenzi MK, da Costa Júnior CT. Fractional Order Pole Placement for a buck converter based on commensurable transfer function. ISA transactions. 2020 Dec 1;107:370-84.

[24] Zúñiga-Aguilar CJ, Gómez-Aguilar JF, Romero-Ugalde HM, Escobar-Jiménez RF, Fernández-Anaya G, Alsaadi FE. Numerical solution of fractal-fractional Mittag–Leffler differential equations with variable-order using artificial neural networks. Engineering with Computers. 2021:1-4.

[25] Sivakumar S, Sathik MJ, Manoj PS, Sundararajan G. An assessment on performance of DC–DC converters for renewable energy applications. Renewable and Sustainable Energy Reviews. 2016 May 1;58:1475-85.

[26] Ahmed G. Radwan, Ahmed A. Emira, Amr M. AbdelAty, Ahmad Taher Azar, Modeling and analysis of fractional order DC-DC converter,ISA Transactions, Volume 82, 2018, Pages 184-199, ISSN 0019-0578, https://doi.org/10.1016/j.isatra.2017.06.024.

[27] Pouzesh M, Mobayen S. Event-triggered fractional-order sliding mode control technique for stabilization of disturbed quadrotor unmanned aerial vehicles. Aerospace Science and Technology. 2022 Feb 1;121:107337.

[28] Zamani AA, Etedali S. Optimal fractional-order PID control design for time-delayed multi-input multi-output seismic-excited structural system. Journal of Vibration and Control. 2023 Feb;29(3-4):802-19.

Ebrahim Abbaszadeh-Soorami is a Ph.D. candidate in Control Engineering, in the Department of Electrical and Robotics, Shahrood university of technology, I.R.Iran. He received his B.Eng. in Electrical-Electronic Engineering, from Azad University branch Lahidjan, I.R.Iran, in 2008 and M.Sc. in Electrical-Control Engineering, from the Shahrood University of Technology, Shahrood, I.R. Iran, in 2013.
Mr. Abbaszadeh's research interests include robotic control, computer numerical control machining, applied computational geometry, fractional-order systems, and discrete-event computer simulation.

Mohammad Haddad-Zarif is Associate Professor of Control Engineering at Shahrood University of Technology, Shahrood, I.R. Iran.
Dr. Haddad-Zarif's research interests include optimal control, robotic control, and applied computational geometry.